Head-to-Toe Measurement of El Gordo: Improved Analysis of the Galaxy Cluster ACT-CL J0102-4915 with New Wide-Field Hubble Space Telescope Imaging Data

Jinhyub Kim[1], M. James Jee[1,2], John P. Hughes[3], Mijin Yoon[4,1], Kim HyeongHan[1], Felipe Menanteau[5,6], Cristobal Sifon[7], Luke Hovey[8], and Prasiddha Arunachalam[3]

[1] Department of Astronomy, Yonsei University
[2] Department of Physics, University of California, Davis
[3] Department of Physics and Astronomy, Rutgers, the State University of New Jersey
[4] Ruhr University Bochum, Faculty of Physics and Astronomy, Astronomical Institute (AIRUB), German Centre for Cosmological Lensing
[5] Center for AstroPhysical Surveys, National Center for Supercomputing Applications, University of Illinois at Urbana-Champaign
[6] Department of Astronomy, University of Illinois at Urbana-Champaign
[7] Instituto de Fisica, Pontificia Universidad Catolica de Valparaiso
[8] Theoretical Design Division, Los Alamos National Laboratory

This poster is a summarized version of Kim et al. 2021 (ApJ submitted; see **arXiv 2106.00031** for detailed descriptions).

contact: jinhyubkim89@gmail.com

Abstract

We present an improved weak-lensing (WL) study of the high-z (z = 0.87) merging galaxy cluster ACT-CL J0102-4915 ("El Gordo") based on new wide-field *Hubble Space Telescope* (HST) imaging data. The new imaging data cover the ~3.5 × ~3.5 Mpc region centered on the cluster and enable us to detect WL signals beyond the virial radius, which was not possible in previous studies. We confirm the binary mass structure consisting of the northwestern (NW) and southeastern (SE) subclusters and the ~2σ dissociation between the SE mass peak and the X-ray cool core. We obtain the mass estimates of the subclusters by simultaneously fitting two Navarro-Frenk-White (NFW) halos without employing mass-concentration relations. The masses are $M_{200c}^{NW} = 9.9^{+2.1}_{-2.2} \times 10^{14}\ M_{sun}$ and $M_{200c}^{SE} = 6.5^{+1.9}_{-1.4} \times 10^{14}\ M_{sun}$ for the NW and SE subclusters, respectively. The mass ratio is consistent with our previous WL study but significantly different from the previous strong lensing results. This discrepancy is attributed to the use of extrapolation in strong lensing studies because the SE component possesses a higher concentration. By superposing the two best-fit NFW halos, we determine the total mass of El Gordo to be $M_{200c} = 21.3^{+2.5}_{-2.3} \times 10^{14}\ M_{sun}$, which is ~23% lower than our previous WL result [$M_{200c} = (27.6 \pm 5.1) \times 10^{14} M_{sun}$]. Our updated mass is a more direct measurement since we are not extrapolating to R_{200c} as in all previous studies. The new mass is compatible with the current ΛCDM cosmology.

Introduction

- Characteristics of ACT-CL J0102-4915 ("El Gordo")
  (1) symmetric double radio relics and two cometary tails in X-ray (Menanteau et al. 2012; Lindner et al. 2014)
  (2) extremely high mass: the most massive at z > 0.5 (Hilton et al. 2021)
  - e.g., $M_{200c} = (27.6 \pm 5.1) \times 10^{14}\ M_{sun}$ (weak-lensing mass; Jee et al. 2014)

- Issues related to El Gordo are
  (1) whether or not the presence of the cluster is in tension with the ΛCDM paradigm (e.g., Harrison & Cole 2012; Katz et al. 2013), and
  (2) details of El Gordo's merging scenario are still uncertain: outgoing vs. returning (e.g., Donnert 2014; Molnar & Broadhurst 2015; Zhang et al. 2015; Ng et al. 2015).

- An accurate mass estimate using weak-lensing (WL) analysis is mandatory to study the compatibility of its existence with the ΛCDM paradigm and to constrain the phase of merger.

- Previous studies using strong and weak lensing analyses relied on extrapolations for their mass measurements because the previous HST observations did not extend out the virial radius of the cluster.

- In this work, we determine an accurate mass measurement of El Gordo without extrapolation using new wide-field HST observations (**Figure 1**).
  - Our new ACS observations in conjunction with archival ACS and WFC3/IR data (24 orbits) cover ~3.5 × ~3.5 Mpc region centered on El Gordo (corresponding to ~119 arcmin^2), ~2.7 times larger than our previous WL field.
  - We detect the WL signal beyond the virial radius of the cluster.

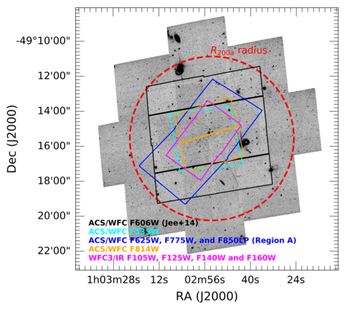

Figure 1. HST observation footprint of El Gordo. The inverted gray scale represents the intensities of ACS/F606W, which covers a total of 119 arcmin^2. Our new ACS/F606W observation with eight pointings surrounds the previous ACS/F606W observation with 2 × 2 mosaic pattern (black), which Jee et al. (2014) used for their weak-lensing analysis. The ACS/F625W, ACS/F775W, and ACS/F850LP data cover a ~6 × 3 arcmin^2 strip with two pointings (blue). The two WFC3/IR pointings (magenta) lie within the strip. ACS/F435W, and ACS/F814W pointings are also indicated. Note that the virial radius (R_{200a}, red dashed line) is enclosed by the new ACS/F606W footprint.

HST Data Reduction and Weak-Lensing Analysis

- HST imaging data: 24 orbits with 4 programs (ID 12477, 12755, 14096, and 14153)
  - 10 ACS and WFC3/IR filters are used (**Figure 1**).

- WL analysis
  - Point spread functions (PSFs) are measured using the PSF library approach (Jee et al. 2007a).
  - Shape parameters are determined by fitting a two-dimensional (2D) elliptical Gaussian model convolved with the appropriate PSF model.
  - Sources are selected by both shape and photometric requirements.

- Readers are referred to our paper (**arXiv 2106.00031**) for details.

Results and Discussions

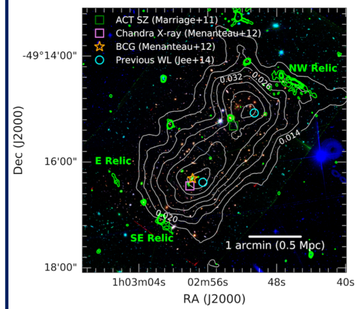

Figure 2. 2D mass reconstruction of El Gordo with the FIATMAP code (Fischer & Tyson 1997). The mass is overlaid on the color composite created with HST F606W (blue), F775W (green), and F105W (red). The symbols represent the centroids measured at various wavelengths. The mass contours start at 2.5σ significance and the significance increases inward by 1σ, reaching peak significance value of ~8.8σ and ~9.0σ for the NW and SE peaks, respectively. The 2.1 GHz ATCA contours are overlaid, which display the three radio relics (Lindner et al. 2014) as well as some bright radio point sources.

Figure 3. Wide-field mass reconstruction of El Gordo. The intensity in purple represents the convergence obtained with the MAXENT code (Jee et al. 2007b). Only for demonstration purpose, here we display 15 arcmin × 15 arcmin color composite created by *g*, *r*, and *z* filters of Dark Energy Camera (Flaugher et al. 2015) for the blue, green, and red channels, respectively. The footprint of our new HST observations is indicated with the yellow solid line. The R_{200a} radius is marked with the yellow dashed line. The center of mass (yellow cross) is computed with the best-fit subcluster masses.

- **Mass reconstruction** (**Figure 2 and 3**)
  - The two subclusters (northwest, NW, and southeast, SE) are detected with a separation of 770 kpc, which is consistent with the previous WL results (Jee et al. 2014; Schrabback et al. 2018).
  - A notable change with respect to the previous WL studies is the mass density enhancement of the SE peak.

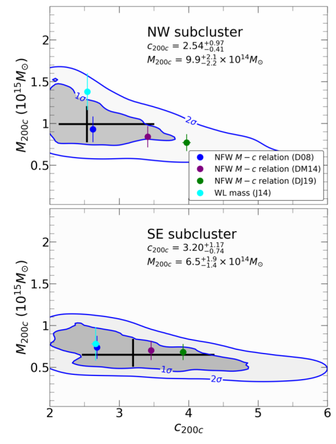

- **Mass estimates** (**Figure 4**)
  - We model the WL signal as a superposition of two halos under the NFW profile.
  - Our main mass results are obtained without mass-concentration (M-c) relation. We use the Bayesian sampling method to determine the mass distribution of El Gordo.
  - The total mass of the cluster is $M_{200c} = 21.3^{+2.5}_{-2.3} \times 10^{14}\ M_{sun}$, which is ~23% lower than our previous WL results (Jee et al. 2014).
  - The mass difference is mainly caused by the increase of the field size (~2.7 times), which enables us to estimate the total mass without any extrapolation.

Figure 4. Posterior distribution from 100,000 MCMC samples of our two-parameter mass determination. The black crosses show the best-fit values and the uncertainties of c_{200c} and M_{200c} after one-dimensional marginalization. For comparison, we display the results when M-c relations are used and our previous WL result (Jee et al. 2014) using Duffy et al. (2008) M-c relation. These fitting results are consistent with the mass estimates obtained from our two-parameter sampling.

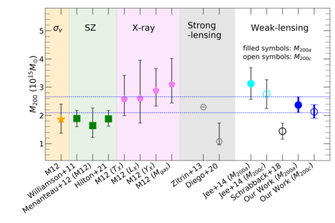

- **Mass comparison with previous studies** (**Figure 5**)

Figure 5. Comparison of mass estimates of El Gordo from various proxies. Our WL mass estimates (M_{200c} and M_{200a}) are statistically consistent with the previous lensing results as well as the proxies that rely on the assumed properties of the gas and galaxies with treating as a single halo. However, the consistency here is due to the large statistical errors. It is worth noting that treating the system as a single halo is an important source of systematics in mass estimation because El Gordo is comprised of two systems with dynamically disrupted structures.

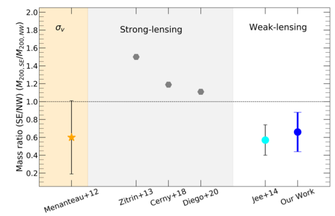

- **Mass ratio: which subcluster is more massive?** (**Figure 6**)

Figure 6. Comparison of the subcluster mass ratio measurements ($M_{200}^{SE}/M_{200}^{NW}$). While strong lensing results (gray hexagons) show that the SE component is more massive, velocity dispersion (orange star) and WL (cyan and blue circles) support the opposite case. We argue that the discrepancy might be due to the SE subcluster mass distribution being more compact. When we crop our WL sources within r < 1.5 Mpc from each mass peak, the SE subcluster is 1.5 ± 0.6 times more massive than the NW one.

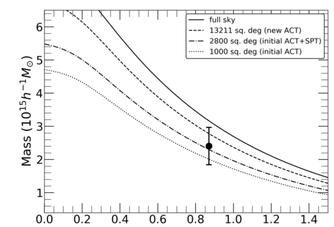

- **Rarity test based on the total mass** (**Figure 7**)

Figure 7. Exclusion curves and mass estimates (M_{200a}) of El Gordo. We display the exclusion curves of 95% (~2σ) confidence level for both sample and parameter variances for the full sky (sold), 13211 deg^2 (dashed), 2800 deg^2 (dash-dotted), and 1000 deg^2 (dotted). The filled circle and its error bar are our WL mass estimate and 2σ statistical uncertainty, respectively. Since El Gordo is below the full sky curve and consistent with the current large-area ACT survey (13211 deg^2; Hilton et al. 2021), the cluster is still rare but is compatible with the prediction of ΛCDM cosmology.